MUTUAL COUPLING REDUCTION TECHNIQUES IN ELECTRONIC STEERING ANTENNAS IN X BAND.

G. Expósito-Domínguez[1], J.M. Fernández-González[1], P. Padilla[2], and M. Sierra-Castañer[1]

[1]*Radiation Group, Signals, Systems and Radiocommunication Department, Universidad Politécnica de Madrid, Ciudad Universitaria, Madrid 28040, Spain.*

[2]*Department of Signal Theory, Telematics and Communications, Universidad de Granada, Periodista Daniel Saucedo Aranda, Granada 18071, Spain.*

ABSTRACT

This work provides the development of an antenna for satellite communications onboard systems based on the recommendations ITU-R S.580-6 [1] and ITU-R S.465-5 [2]. The antenna consists of printed elements grouped in an array, working in a frequency band from 7.25 up to 8.4 GHz (15% of bandwidth). In this working band, transmission and reception are included simultaneously. The antenna reaches a gain about 31 dBi, has a radiation pattern with a beamwidth smaller than 10º and dual circular polarization. It has the capability to steer in elevation through a Butler matrix to $45°$, $75°$, $105°$ and $135°$ electronically and $360°$ in azimuth with a motorized junction. In order to enhance the features of the antenna, mutual coupling reduction techniques based in Electromagnetic Band Gap (EBG) were studied.

Key words: Steering antenna; Mutual coupling reduction; EBG.

1. INTRODUCTION

The increasing use of broadband satellite systems to provide ubiquitous and high-capacity communications demands lightweight, low-profile steerable-beam antennas with a small footprint that can be integrated on vehicles, trains or aircrafts. Therefore, a necessity of more demanding mobile satellite terminals is emerging. These terminals require antenna frontends capable of tracking one or more satellites (uni/bidirectional) and provide at the same time sufficient band width. X band satellite is widely available and can easily provide rich multimedia broadcasting as well as broadband communications services at a competitive cost with respect to other satellite systems at lower frequencies. However, X band antenna terminals are generally expensive and heavy, while phased array technology can provide low-profile and reliable solutions at a reasonable price for mass production.

The aim of this work is the development of an onboard satellite communications system in X band. This printed antenna has the following capabilities: broadband capacity (7.25 - 8.15 GHz) 15%, dual circular polarization (RHCP and LHCP, interchangeable for transmission (TX) and reception (RX), good axial ratio (AR $<$ 3dB) and beam steering ($90°$ elevation) by means of a passive Butler network matrix. Table 1 provide the complete design specifications for this antenna.

Table 1. Antenna specifications.

Parameter	Value	Comments
Polarization RX	LHCP	Left Handed Circular Polarization*.
Polarization TX	RHCP	Right Handed Circular Polarization*.
Gain	31 dBi	For the broadside direction.
Maximum Dimensions	$<$0.6 m	Equivalent diameter.
Antenna Efficiency	$>$60%	Including network losses.
Axial Ratio	$<$3 dB	Circular polarization purity.
CP/XP	$>$25 dB	Co-polar and Cross-polar Ratio.
S_{11}	$<$-15 dB	Reflection coefficient.
S_{21}	$<$-15 dB	Isolation between frequency bands.

*Both are interchangeable.

This paper is organized as follows. Section 2 shows the process design of the antenna in three stages, the design of the array, the sub array and the steering network features. In section 3, complete prototypes are shown and measured. Section 4 is devoted to the study of mutual coupling reduction based on Electromagnetic Band Gap (EBG). Finally, in Section 5 the conclusions are drawn.

2. SYSTEM DESIGN

This antenna has been designed in two main different parts: the radiating element, an array of printed microstrip antennas and a passive Butler network based in hybrid couplers, which gets the necessary phase shift in order to obtain the steering direction. A rectangular structure of 16x24 elements has been selected [3]. These elements are treated in two different ways:

- Rows: First grouped in rows, separated a distance between them of $0.85\lambda|_{7.25\ GHz}$.
- Columns: Thus, 16 rows of 24 elements are grouped and separated $0.5\lambda|_{7.25\ GHz}$. The steering direction of the main beam is achieved due to the phase shifting between each row.

2.1. Sub array

In order to handle the problems that this complex system presents, it is decided to split the system. The antenna is based in a 4x4 circular microstrip patches sub array [4]. This elements are treated in two different ways. First, 4 radiating elements grouped in rows, with a separation between them of $0.85\lambda|_{7.25\ GHz}$ in order to increase the effective area of the antenna. Those elements are fed by a uniform passive distribution network. Secondly, 4 rows are grouped vertically with a separation of $0.5\lambda|_{7.25\ GHz}$, with this separation the grating lobes in electronic steering radiation angles are avoided (Fig.1).

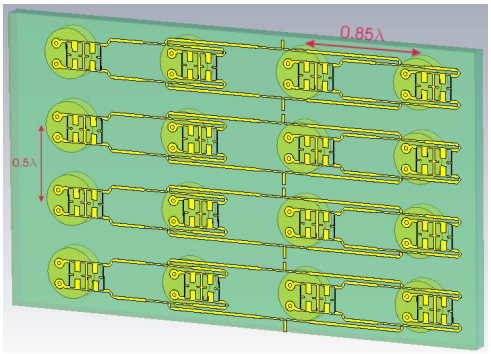

Figure 1. Array simulation.

The radiating element is composed of an array of two-stacked patches: the upper one is fed by electromagnetic coupling, and the bottom one, is fed by two via holes to get the circular polarization. A two stages miniaturized hybrid coupler [5] enhances the bandwidth of the circuit, permits two circular polarizations(RHCP and LHCP) at the same time, and increases the isolation between both channels (TX and RX). In the bottom part of the antenna, the feeding distribution network and connectors are placed. The substrate permittivity is 2.17 in order to get good radiation of the antenna. Despite reducing Q factor, the substrates and foam thickness are thick in order to enhance the bandwidth ($\sim 15\%$) [6].

2.2. Butler Matrix

The Butler matrix is a passive network with 2^n inputs, 2^n outputs, $2^{n-1}log_2 2^n$ hybrid couplers, crossovers and phase shifters [7]. The function of a Butler matrix is to combine signals in phase to or from an antenna array. It produces 2^n beams with constant angular separation. Each output signal S_n it can be expressed as follows (1).

$$S_n = \sum_{m=1}^{n} A_m e^{j\alpha_{mn}} \tag{1}$$

where A_m is the input signal in *m* port and α_{mn} is the phase difference between input ports. In this work a Butler matrix with 4 inputs and 4 outputs has been designed. The output phase difference is $\pm 45^\circ$ and $\pm 135^\circ$, and crossovers are implemented with two hybrid couplers in cascade.

The hybrid coupler is the key design part since the rest of the elements are based on it. This hybrid coupler is designed in two stages, in order to enhance the bandwidth of the device. Crossovers, are compound of two hybrid couplers in cascade. This passive circuit allows to cross different lines in the substrate without using multilayered structures with good isolation. Therefore, the signal that enters through port 1 goes out through port 4, meanwhile the signal in port 3 it is canceled because its components has a π phase difference. Likewise, signal in port 2 goes to port 3 and it is cancelled in port 4. Phase shifters are based in transmission lines, which introduce a phase shifting of 45°, as well as they compensate the electrical length of crossovers.

3. CONSTRUCTION AND MEASUREMENTS

An antenna prototype has been built to measure the radiation patterns and to verify the antenna performances.

3.1. Array

Firstly, Fig. 2 shows the bottom part of the construction of the 16 elements subarray. This figure, shows the top patches, which are fed by electromagnetic coupling and the connectors, which will be connected to the steering network. If the Butler matrix is connected to left side ports, the antenna radiation will be LHCP and viceversa. The rest of the ports will be charged with 50Ω loads.

The S parameters of eight input ports of the sixteen elements array are presented in Fig. 3. The continuous line shows the left side ports, the dashed line represents the right side ports and the marked line points to the isolation between two ports together. The isolation is adecuate, with a value under 15 dB for the whole band ($S_{RL} < -15$ dB) and the reflection coefficient for all the ports is under 10 dB ($S_{ii} < -10$ dB).

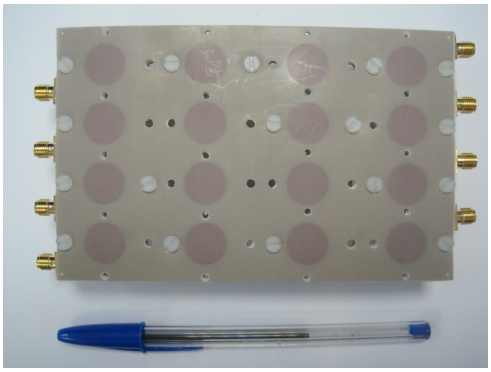

Figure 2. Multilayered array construction.

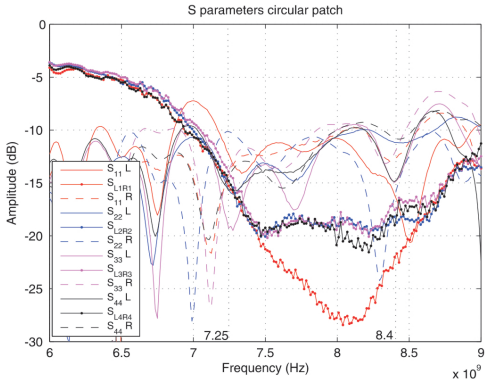

Figure 3. S parameters of 4x4 array (8 ports).

3.2. Steering network

Fig. 4 shows the Butler matrix. In this figure, the prototype and each of its parts it is shown [8]. The hybrid coupler and the phase shifters are based on transmission lines. Crossovers are implemented in one layer with a double hybrid coupler in cascade. This circuit is electrically large and it can not be included in the same layer of the distribution network. For that reason, it is built in a different printed circuit board. Nevertheless, in this way, it can be used for both TX and RX.

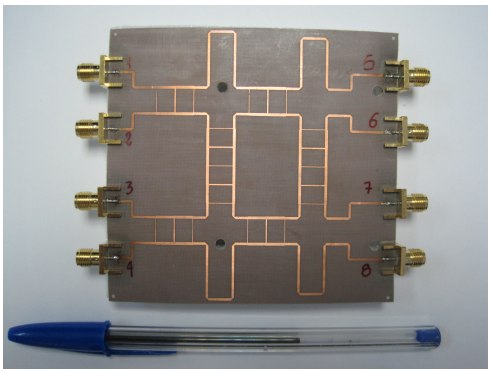

Figure 4. Butler matrix construction.

The amplitude of the Butler matrix S parameters is presented in Fig. 5. Theoretically, the output power distribution is -6 dB in each port. However, due to the fabrication process, reflection coefficients, losses, and the isolation of the circuits the output distribution is -6.5 ± 2 dB (continuous line). The final isolation between ports is better than 12 dB (dashed line).

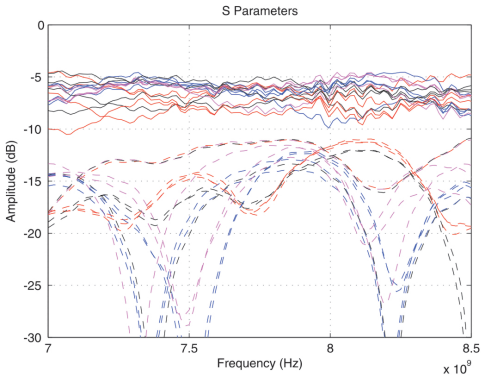

Figure 5. S parameters in amplitude of Butler matrix.

In Fig. 6 and Fig. 7, the output phase are shown. It can be seen that the simulations (dashed line) are in good agreement with measurements (continuous line). When input signal enters in port 1 (see Fig. 4)the phase difference between the outputs is $-45 \pm 5^\circ$ (Fig. 6). Fig. 7 shows the phase difference between the outputs $+135 \pm 5^\circ$ when the input signal enters through port 2, and the other inputs are loaded with 50Ω. Similar results are obtained for ports 3 and 4, with phase differences of $-135 \pm 5^\circ$ and $+45 \pm 5^\circ$ respectively.

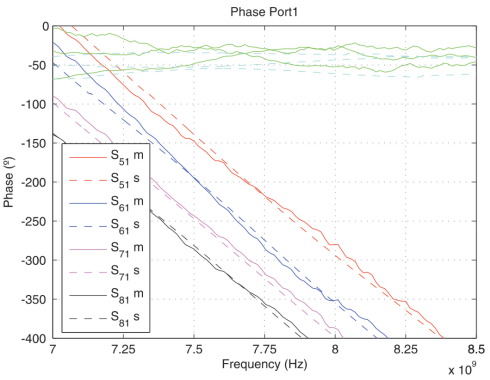

Figure 6. S parameters in phase of Butler matrix (Port1).

3.3. Subarray Measurements

Fig. 8 shows the measurement setup of the complete system. In it, the 16 element array and the Butler matrix are connected through low losses cables. The 4x4 subarray has been measured at the facilities of Technical University of Madrid (UPM).

In Fig. 9 and Fig. 10 the radiation patterns of the steering antenna are shown for the center frequency of each band

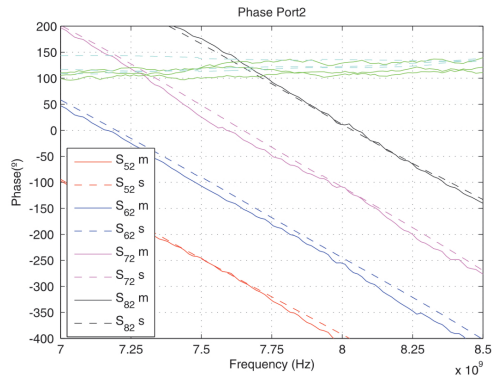

Figure 7. S parameters in phase of Butler matrix (Port2).

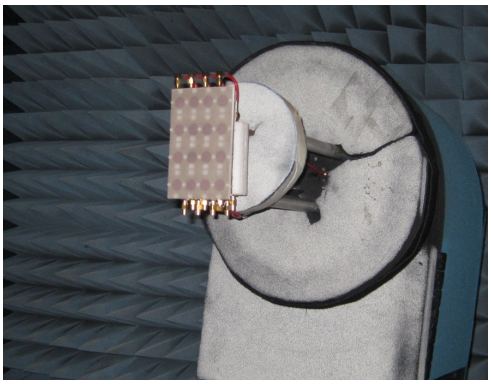

Figure 8. Measurement setup in the anechoic chamber.

(7.25 GHz and 8.15 GHz). The steering angles $-45°$, $-15°$, $15°$ and $45°$ correspond to a phase difference feed $\alpha = 135°$ (purple), $\alpha = 45°$ (red), $\alpha = -45°$ (black)and $\alpha = -135°$ (blue) respectively. The marked line presents the measured data, while the dashed line shows the simulated data, which are in good agreement. The cross polar component is represented in continuous line.

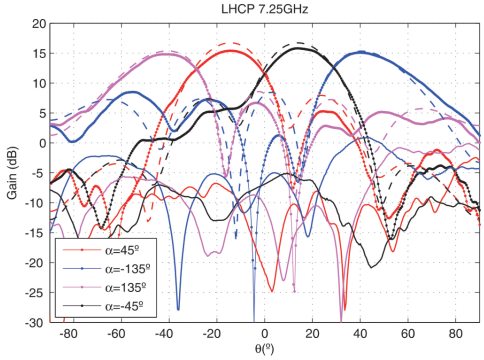

Figure 9. Steering radiation pattern (LHCP 7.25 GHz) measurement vs simulation.

It can be seen, in both figures (Fig. 9 and Fig. 10), a gain reduction in the main beam in directions far from the broadside. This is reasonable due to the main beam widening. The level differences between measurements (marked line) and simulations (dashed line) are because the cable and connector losses were not taken into account.

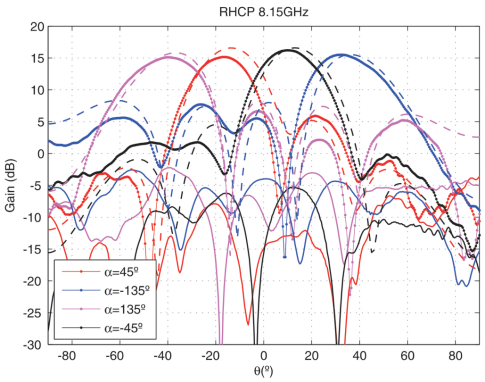

Figure 10. Steering radiation pattern (RHCP 8.15 GHz) measurement vs simulation.

The axial ratio of the main beams, ($-45°$, $-15°$, $15°$ and $45°$) for the different frequencies and different polarizations (LHCP$_{7.25GHz}$ and RHCP$_{8.15GHz}$), are under -3 dB for each pointing beam $\pm 25°$.

The CP/XP is larger than 20 dB in the main beam for the different steering directions. As expected, the values of circular polarization purity for the main beam are under 1 dB.

4. SURFACE WAVE EFFECT SUPPRESSION

Due to the use of the thick substrate, in order to cover the whole band (1.15 GHz), the surface-wave propagation effect appears. This effect yields a negative contribution in mutual coupling and isolation between elements. To solve this problem, different solutions are taken into account: cavity patches, Defected Ground Structure (DGS), etc. although periodic planar Electromagnetic Band Gap (EBG) these EBG seems to be the best solution due to compactness and feasibility of construction (Fig. 11).

EBG technique appears as an application of truncated frequency selective surface (FSS) [9]. These structures consist of an array of metal protrusions on a flat metal sheet and can be visualized as mushrooms protruding from the surface. When the period is small compared to the wavelength of interest, it is possible to analyze the material as an effective medium, with a surface impedance. These ”mushrooms” present very high impedance for vertical an horizontal modes at certain frequencies.

These structures can be analyzed as resonant LC circuits, in which the capacitance is provided by the proximity of the metal plates, and the inductance is related to the thickness of the structure. Therefore, the surface impedance is given by the following expression:

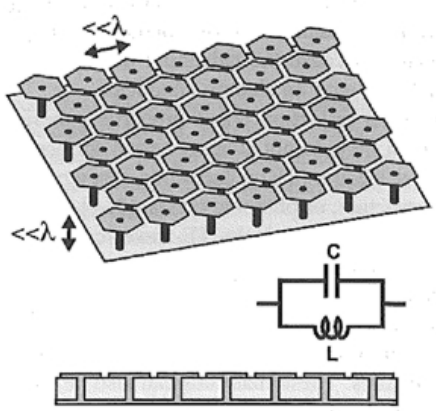

Figure 11. High impedance surface and its model with parallel resonant LC circuit [9].

$$Z_s = \frac{j\omega L}{1 - \omega^2 LC} \tag{2}$$

The resonance frequency of the circuit is given by:

$$\omega_0 = \frac{1}{\sqrt{LC}} \tag{3}$$

Below resonance, the surface is inductive meanwhile above resonance, the surface is capacitive. Near ω_0, the surface impedance is much higher than the impedance of free space [10].

In this work, EBG structures are used in order to reduce the mutual coupling between elements [11]. To study this effect, a simulation scheme is prepared with a transmission line whose ground plane is replaced by an EBG plane (Fig. 12). This simulation was carried out for different patch sizes *w*, and different number of periods *n*.

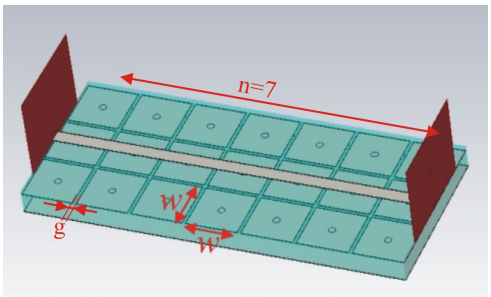

Figure 12. EBG simulation scheme.

From Fig. 13 results, the dimensions of the patch to avoid field propagation in the working frequency band (7.25 - 8.4 GHz)is extracted. The best value is 3.15 mm approximately and the minimum number of mushrooms should be $n = 4$ (Fig. 14). The vertical separation between rows is $0.5\lambda|_{7.25\ GHz}$ (20.8 mm) and the size of the patch for

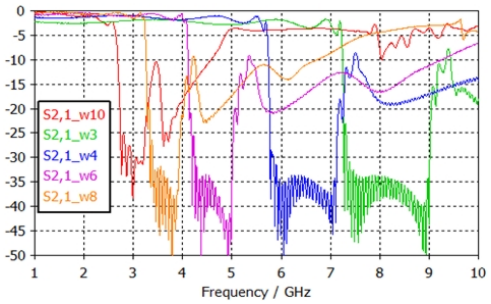

Figure 13. Transmission coefficient for a transmission line with EBG ground plane.

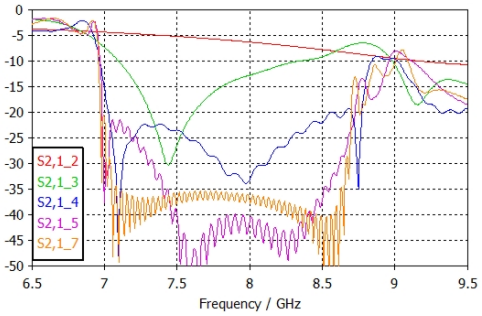

Figure 14. Transmission coefficient for different number of mushrooms n.

$\epsilon_r = 2.17$ is 13.7 mm, thus the separation between elements is 7 mm. Therefore the available space is not enough for two rows of elements. Consequently other alternatives have to be taken into account. The solution needs to reduce the size of the mushroom patch, but maintaining the capacity of the equivalent circuit. This can be done by changing the shape of the patch (Fig. 15), or by using multilayered EBG surface (Fig. 16). Since the bandwidth is proportional to $\sqrt{L/C}$, for a fixed thickness the higher the capacity is, the lower the operation bandwidth is. Therefore solutions based in capacity increasing inevitably reduce the operation of the EBG structure.

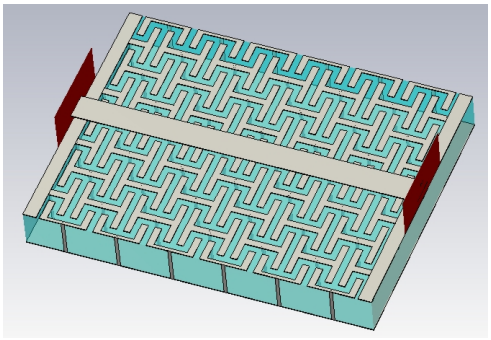

Figure 15. H EBG shape.

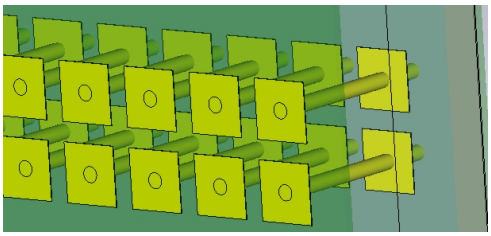

Figure 16. Multilayered EBG.

5. CONCLUSIONS

In this work, a wide band printed antenna with electronic steering capability has been presented. Its parts, feeding distribution network, hybrid coupler and Butler matrix have been developed in order to get wideband, two circular polarizations (RHCP and LHCP) and a good isolation between transmission and reception band. This design is validated with the construction and measurements of the whole antenna. Finally, a preliminary study for mutual coupling reduction based on EBG structures was carried out. Further results will be presented in 33^{rd} ESA Antenna Workshop on Challenges for Space Antenna Systems.

ACKNOWLEDGMENTS

The simulations done in this work has been carried out using CST Microwave Studio Suite 2011 under a cooperation agreement between Computer Simulation Technology (CST) and Universidad Politécnica de Madrid. We kindly thank the company NELTEC S.A. for giving the substrates, in which the prototypes were built, freely. This work is been supported by an UPM grant CH/003/2011, the project CG10-UPM/TIC-5805 and the CROCANTE project with reference TEC2008-06736-C03-01.

REFERENCES

1. ITU-R. Radiation diagrams for use as design objetives for antennas of earth station operating with geostacionary satellites. Recommendation 580-6, International Telecommunication Union, 2004.

2. ITU-R. Reference earth-station radiation pattern for use in coordination and interference assessment in the frequency range from 2 to about 30 ghz. Recommendation 465-5, International Telecommunication Union, 1993.

3. G. Expósito-Domínguez, P. Padilla-Torre, J. M. Fernández-González, and M. Sierra-Castañer. Electronic steering antenna onboard for satellite communications in x band. 5^{th} *European Conference on Antennas and Propagation (EuCAP 2011)*, pages 2120–2123, Apr. 2011.

4. J. R. James and P. S. Hall. *Handbook of Microstrip Antennas*. IEEE waves series, 1989.

5. C. W. Tang and M. G. Chen. Synthesizing microstrip branch-line couplers with predetermined compact size and bandwidth. *IEEE Trans on Microwave Theory and Techniques*, 55(9):1926–1934, 2007.

6. A. García-Agilar, J. M. Inclán-Alonso, J. M. Fernández-González, and M. Sierra-Pérez. Printed antenna for satellite communications. *2010 IEEE International Symposium on Phased Array Systems and Technology*, pages 529–535, Oct. 2010.

7. J. Butler and R. Lowe. Beam-forming matrix simplifies design of electronically scanned antennas. *Electronic Design*, 9:170–173, 1961.

8. G. Expósito-Domínguez, P. Padilla-Torre, J. M. Fernández-González, and M. Sierra-Castañer. Matriz de butler de banda ancha en banda x para antenas reconfigurables. *XXV URSI Spain*, Sep. 2011.

9. D. Sievenpiper, L. Zhang, R. Broas, N. Alexopoulos, and E. Yablonovitch. High-impedance electromagnetic surfaces with a forbidden frequency band. *IEEE Trans. On Microwave Theory and Techniques*, 47:2059–2074, Nov. 1999.

10. F. Yang and Y. Rahmat-Samii. *Electromagnetic Band Gap Structures in Antenna Engineering*. The Cambridge RF and Microwave Engineering Series, 2008.

11. E. Rajo-Iglesias, O. Quevedo-Teruel, and L. Inclán-Sánchez. Mutual coupling reduction in patch antenna arrays by using a planar ebg structure and a multilayer dielectric substrate. *IEEE Trans. on Antennas and Propagation*, 56(6):1648–1655, Jun. 2008.

12. R. Garg, I. bahl, and A. Ittipiboon. *Microstrip Antennas Design Handbook*. Artech House, 2001.

13. G. Matthaei and L. Young. *Microwave Filters, Impedance-Matching Networks, and Coupling Structures*. Artech House Publishers, 2000.

14. D. M. Pozar and D. H. Schaubert. *Microstrip Antennas: The analysis and design of microstrip antennas and arrays*. IEEE press, 1995.

15. A. García-Agilar, J. M. Inclán-Alonso, J. M. Fernández-González, and M. Sierra-Pérez. Printed antenna for satellite communications. 4^{th} *European Conference on Antennas and Propagation (EuCAP 2010)*, Apr. 2010.

16. Fan Yang and Y. Rahmat-Samii. Microstrip antennas integrated with electromagnetic band-gap (ebg) structures: a low mutual coupling design for array applications. *Antennas and Propagation, IEEE Transactions on*, 51(10):2936–2946, Oct. 2003.

17. T. Itoh C. Caloz. *Electromagnetic metamaterials: transmission line theory and microwave applications : the engineering approach*. John Wiley and Sons, 2006.